

OxBioZ: Wearable Continuous Bioimpedance Monitoring System and Multi-Activity Dataset with Physiological and Motion Signals

Xinyu Hou
University of Oxford
Oxford, UK

Yiyuan Yang
University of Oxford
Oxford, UK

Jonas Beuchert
Cardiff University
Cardiff, UK

Hakan Kayan
Cardiff University
Cardiff, UK

Qian Xie
University of Leeds
Leeds, UK

Kim Tien Ly
University of Oxford
Oxford, UK

Qianyi Deng
University of Oxford
Oxford, UK

Nhat Pham
Cardiff University
Cardiff, UK

Andrew Markham
University of Oxford
Oxford, UK

Niki Trigoni
University of Oxford
Oxford, UK

Abstract

Vital sign monitoring and body composition analysis are both used for various medical applications. However, there is a lack of devices capable of conducting continuous vital sign monitoring and body composition analysis simultaneously during daily activities. We present a wearable device named 'OxBioZ', capable of performing (i) continuous single-frequency bioimpedance analysis, (ii) multi-frequency bioimpedance analysis, (iii) electrocardiography (ECG), and (iv) inertial measurements. This allows continuous estimation of cardiac function, respiration analysis and total body water (TBW) during daily activities without the needs for multiple devices or specialized monitoring protocols. Leveraging OxBioZ, we collected a comprehensive multi-activity dataset from 21 participants, totaling over 1000 min of synchronized bioimpedance, motion, and ground-truth physiological measurements. Baseline studies on vital sign estimation and TBW assessment demonstrate the platform's feasibility and provide a benchmark dataset for advancing bioimpedance-driven wearable health analytics.

CCS Concepts

• Applied computing → Consumer health.

Keywords

Biosignal, Bioimpedance, Wearable devices

ACM Reference Format:

Xinyu Hou, Yiyuan Yang, Jonas Beuchert, Hakan Kayan, Qian Xie, Kim Tien Ly, Qianyi Deng, Nhat Pham, Andrew Markham, and Niki Trigoni. 2025. OxBioZ: Wearable Continuous

Bioimpedance Monitoring System and Multi-Activity Dataset with Physiological and Motion Signals. In *3rd ACM Workshop on Smart Wearable Systems and Applications (SmartWear '25)*, November 4–8, 2025, Hong Kong, China. ACM, New York, NY, USA, 6 pages. <https://doi.org/10.1145/3737903.3768566>

1 Introduction

Continuous monitoring of physiological signals is critical for diverse domains, ranging from medical diagnostics [7], chronic disease management [3], and telemedicine [14] to emergency response [17]. Body composition analysis, which quantifies parameters such as fat mass, muscle mass, and total body water (TBW) [12], provides complementary insights into an individual's health status and functional capacity. In many high-stakes scenarios—e.g., monitoring firefighters to prevent heat-related injuries—both continuous vital sign tracking (e.g., heart rate, breathing rate) and body composition assessment (e.g., TBW) are required simultaneously. However, existing solutions typically target either physiological signal monitoring or body composition estimation, and often rely on bulky, non-wearable systems, limiting their applicability in daily-life or work environments. More noninvasive, unobtrusive, and lightweight options include consumer-grade wearables such as smartwatches [8] and patches [13], yet they seldom support body composition analysis alongside continuous vital-sign monitoring.

To address this gap, we present OxBioZ, a wearable, unobtrusive sensing platform capable of capturing multi-modal physiological and motion signals in real time. OxBioZ integrates: (i) continuous single-frequency bioimpedance, (ii) multi-frequency bioimpedance sweeps, (iii) electrocardiography (ECG), and (iv) inertial measurements, enabling both vital sign analysis and body composition estimation without the need for multiple devices or special monitoring setups.

Leveraging this platform, we collected a comprehensive multi-activity dataset from 21 participants, totaling over 1000 min of synchronized bioimpedance, inertial, and ground-truth physiological measurements. We showcase its potential



This work is licensed under a Creative Commons Attribution 4.0 International License.

SmartWear '25, Hong Kong, China

© 2025 Copyright held by the owner/author(s).

ACM ISBN 979-8-4007-1980-6/2025/11

<https://doi.org/10.1145/3737903.3768566>

through baseline evaluations spanning both frequency-based and sequence-based physiological monitoring, as well as body composition estimation. These studies validate the feasibility of OxBioZ for a broad spectrum of wearable health analytics and establish a benchmark resource for future research in bioimpedance-driven sensing.

2 Background

Bioimpedance refers to the electrical properties (resistance and reactance, specifically) of biological tissue, which can be measured by applying a known current to a biosample and recording the voltage drop. The resistance in bioimpedance comes mainly from extracellular and intracellular fluids, while cellular membranes act similarly to capacitors [11]. Different body compositions result in distinct bioimpedance values, making it a widely used noninvasive method.

Bioimpedance measurements are commonly performed using tetrapolar impedance sensors with one pair of electrodes for current injection and another pair for the voltage drop measurement. The separation of injection and measurement electrode pairs helps to minimise the impact of fluctuating contact impedance between the electrodes and the skin [18].

Different current frequencies are used for bioimpedance measurements because tissues and their components (e.g., cells and fluids) respond differently to varying frequencies [12].

Bioimpedance can be used to estimate TBW as an indicator of hydration [15]. This method is based on the concept that body tissue can be modeled as an electrical circuit consisting of resistances and capacitance [10]. It has been validated to be as accurate as blood sampling techniques in measuring acute hydration changes [9]. Current medical-grade bioimpedance analysers normally use eight electrodes on ankles and wrists, which requires a complex setup and cannot be measured continuously in real-time.

Wearable hydration monitoring devices on the market use, e.g., hand-to-hand bioimpedance via wristbands to estimate body water levels [1], though this method requires manual contact for 30 seconds and cannot support real-time or activity-based monitoring.

3 Hardware

We place the electronic components for acquiring, processing, and transmitting the biosignal data on a series of printed circuit boards (PCBs), see Figure 1. All PCBs are small, measuring only $37\text{ mm} \times 22.5\text{ mm}$ or less. This form factor allows the electronics to be worn unobtrusively.

3.1 Data Collection System

The first PCB comprises the electronics necessary for bioimpedance data acquisition. The bioimpedance analog front-end (BioZ AFE) is a low-power ANALOG DEVICES MAX30009

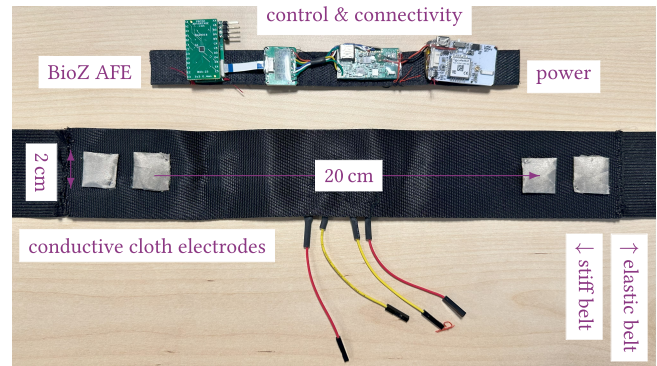


Figure 1: Trunk-facing side of measurement belt.

integrated circuit (IC). It measures $2\text{ mm} \times 2\text{ mm}$. In addition to its small form factor, its low power consumption of about $250\text{ }\mu\text{W}$ renders it particularly suitable for a wearable, battery-powered device. Four electrodes are wired to the data acquisition PCB. The two outer electrodes are connected to an AC current source that is part of the MAX30009. They apply a sinusoidal stimulation current with a root-mean-square (RMS) value of up to 1 mA and a frequency of 51 200 kHz in regular intervals. The two inner electrodes are connected to the analog front end of the MAX30009 IC. The signals are high-pass filtered and amplified using an instrumentation amplifier. Since the measurements are done for AC stimulation signals, the measurement signals are differential signals and require the removal of DC and low-frequency AC signals. A demodulator splits the signals from the two measurement electrodes into a real and an imaginary (I and Q) signal to facilitate the measurement of the complex impedance. The same process also down-converts the signal frequency to DC. These analog DC signals are then sampled and digitised by a 20-bit analog-to-digital converter (ADC) for the I and Q signal, respectively. Their sampling frequency is 200 Hz . For a stimulation current with a given amplitude, the measured DC voltage is proportional to the real and imaginary part of the bioimpedance, respectively. Before data acquisition, we calibrate the AFE using an on-board resistor. We use a single resistor to calibrate both, the I and the Q channel. We first programmatically connect it to the I channel and then to the Q channel. For each channel, we estimate a fixed offset as well as scaling coefficients for the magnitude and phase.

The BioZ AFE PCB is connected to a second PCB, see Figure 1, which has a microcontroller (MCU) that schedules the data acquisition and transmission. The BioZ AFE connects to the MCU via a Serial Peripheral Interface (SPI). The MCU buffers the measurement data and sends it in real-time via a Bluetooth® Low Energy (BLE) connection to a PC.

A rechargeable lithium-ion polymer battery powers both aforementioned PCBs. It is permanently connected to a PCB

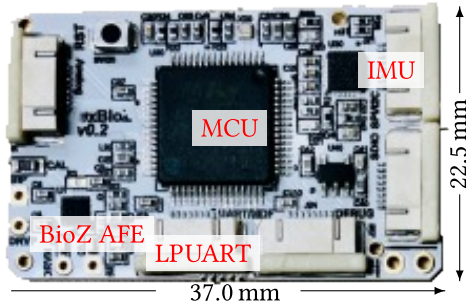


Figure 2: Custom-made OxBioZ v0.2 board combining bioimpedance analog front-end (BioZ AFE), inertial measurement unit (IMU), and microcontroller (MCU).

with a charging circuit and a USB connector for power supply while charging. We choose lithium-ion polymer batteries with 250 mA h to 320 mA h capacity. One powers the entire belt during several hours of continuous data acquisition.

We collect inertial data from the trunk, 3D accelerometer and 3D gyroscope data, to be specific. We use either a STMICROELECTRONICS LSM9DS1 or a BOSCH BMI270 internal measurement unit (IMU) operating at 60 Hz, respectively, and transmit the data in real time via BLE to a PC, too.

3.2 Belt

The wearable belt that holds the measurement electronics is shown in Figure 1. For the experiments, we use two different electrode setups. For most of the data collection, we employ commercial foam gel electrodes (SKINTACT[®] FS-TC1/10up), which are widely used for monitoring electrical biosignals in clinical applications. This choice aids the generalisability of the published dataset. We choose 20 cm for the distance between the measurement electrodes because the apex of the heart (the most inferior, anterior, and lateral part of the heart) usually lies 10.5 cm to 11.5 cm from the midsternal line [16]. Therefore, the center of the heart will be located between the electrodes, allowing for the capture of strong heart signals in the sensed data, signals of potential interest. In addition, we also collect some data with a novel design consisting of electrodes made of woven conductive fabric (SHZHOU WANHE ELECTRONIC CO., LTD. PT230), see Figure 1. We cut a 2 cm × 2 cm piece of cloth for each of the four electrodes and sew it with conductive stainless thread (DFROBOT FIT0743) to the belt. We pad the space between the electrode fabric and the belt with a 5 mm layer of visco-elastic cool gel memory foam (HANSON AND LANGFORD B08LF42W4G) [4]. The belt electrodes have the advantage comparing to gel electrodes that they are reusable, washable, and easier to wear. A central inelastic segment keeps the distance between the electrodes and, hence, the length of the current path approximately constant. This reduces the bioimpedance noise introduced

by varying electrode placement. The distances are the same as the gel electrodes’ distances. The remainder of the belt is stretchable to adjust to the subject’s chest circumference.

3.3 Combined BioZ AFE, IMU, and MCU

We executed the data collection in Section 4 using the electronics described in Section 3.1. Encouraged by the results, we also developed a single small PCB that integrates BioZ AFE, IMU, and MCU, see Figure 2. The electronics are built around an STMICROELECTRONICS STM32U575RI MCU with an Arm[®] Cortex[®]-M33 core, which is a capable processor with a 32-bit floating point unit allowing the implementation of complex signal processing routines. However, the low power consumption of the MCU still allows for extended battery-powered operation, which is crucial for a wearable continuous monitoring system. The MCU acquires accelerometer and gyroscope measurements from a low-power TDK INVENSENSE ICM-20948 IMU via I2C. The bioimpedance analog front-end is the low-power MAX30009 IC, which we already describe in Section 3.1 and is connected to the MCU via an SPI interface. In addition to I2C and SPI, the PCB also exposes the MCU’s serial wire debug (SWD) interface for programming the device, a low-power UART (LPUART) interface for inter-board communication with a wireless connectivity board, and a standard UART interface for debugging.

The firmware for the MCU is entirely written in C++. It acquires the data with the same sampling frequency as the prototype belt described in Section 3.1 and also includes a BioZ AFE calibration routine as described in Section 3.1. When continuously acquiring and streaming BioZ and IMU data at 200 Hz via Bluetooth, the current consumption is about 43 mA at 3.7 V supply voltage. The chosen lithium-ion polymer batteries have a maximum charge of up to 320 mA h. Hence, data acquisition could last for more than 7 h. Overall, this PCB is small, measuring only 37 mm × 22.5 mm, allowing for even less obtrusive continuous monitoring while providing a powerful platform for onboard signal processing.

4 Dataset

We use our system to record over 1000 min of trunk bioimpedance together with various physiological and motion signals of 21 subjects performing a range of different daily activities. The dataset can be found at <https://github.com/XinyuHou97/OxBioZ>. All subjects gave their informed consent for the study, which has been approved by the Research Ethics Committee of the Department of Computer Science of the University of Oxford. Statistics about the physical characteristics are provided together with the dataset.

Table 1: Additional data collection devices.

Sensor type	Sensor model	Frequency	Data
Spirometer	Go Direct Spirometer Vernier	50 Hz	Volume, Differential pressure Adjusted volume, Cycle volume Respiration rate, Flow Rate
IMU	Arduino Nano 33 BLE Sense	60 Hz	3-axis acceleration 3-axis angular velocity
Oximeter	Apple watch	0.2 Hz	Heart rate
BCA	mBCA 525 Seca	-	Total body water (TBW) Extra cellular water (ECW) Fat / muscle mass, etc...
ECG	Heal Force ECG Monitor	-	3-lead ECG signal

Table 2: Data collection protocol.

Period	Time	Device	Description
Measure 1	-	BCA	Measure body composition with BCA.
		BioZ AFE	Measure MF-BIA with BioZ AFE at 12 frequencies ($F_I = 819200, 409600, 204800, 102400, 51200, 25600, 12800, 6400, 3200, 1600, 800, 40$ Hz). Measure weight.
Short test 1	5 min	BioZ AFE	Five 1-min activities:
		IMU	lying, sitting, standing, walking, running.
		Oximeter	BioZ AFE collects in single-frequency mode
		Spirometer	SF-BIA: $I = 32.00 \mu\text{Arms}$, $F_I = 51$ 200 Hz .
Long test 1	20 min	BioZ AFE	0-3 min: warm-up, (walk 6 km/h).
		IMU	3-17 min: walk/jog/run at set speed.
		Oximeter	17-20 min: cool-down (reduce speed).
			Record Borg Rated Perceived Exertion (RPE) score.
Measure 2	-	Same as Measure 1	
Long test 2	20 min	Same as Long test 1	
Short test 2	5 min	Same as Short test 1	
Measure 3	-	Same as Measure 1	

4.1 Devices

For the large-scale data collection, we used the OxBioZ together with gel electrodes on 20 subjects, to ensure a better signal-to-noise ratio for wider applications and more different electrode types in future research. On one subject, we tested the fabric cloth electrodes. In addition, we employed a spirometer, a pulse oximeter, a body composition analyzer (BCA), and an ECG to collect additional physiological signals and ground truth, see Table 1.

4.2 Protocol

Before data collection, subjects completed Perceived Functional Ability (PFA) and Physical Activity Rating (PAR) questionnaires. The scores also determined the assigned running speed in the following experiments. Next, height and circumferences were measured. Then a 1-min ECG signal was collected with both, the ground-truth ECG device and OxBioZ, together at the same time. The following multi-activity experiments are listed in Table 2. If the average PFA1 and PFA2 score of the subject was in the range of 1-5, speed 6.5 km/h was adopted in the long test's running phase; in the range of 5-11, speed 8 km/h; in the range of 11-13, speed 12 km/h. After each long test, subjects were shown a 0-10 Borg rating form of Rated Perceived Exertion (RPE) [2] and asked to choose the score that matches their fatigue status.

Figure 3 shows a subject in a data collection phase where gel electrodes are used together with the OxBioZ electronics and another subject wearing the OxBioZ belt in the same experiment phase.

5 Sample Tasks on Dataset and Device

We present several sample tasks to demonstrate the capabilities of both the OxBioZ device and the associated dataset.

5.1 ECG Signal Recording

The OxBioZ device is capable of recording ECG signals by disabling the demodulation current output and directly measuring the heart's electrical activity. Figure 4 shows a comparison between ECG signals recorded simultaneously by OxBioZ and a professional 3-lead ECG device. The P wave, QRS complex, and T wave are clearly visible in the OxBioZ recordings, demonstrating the device's ability to capture high-quality ECG data.

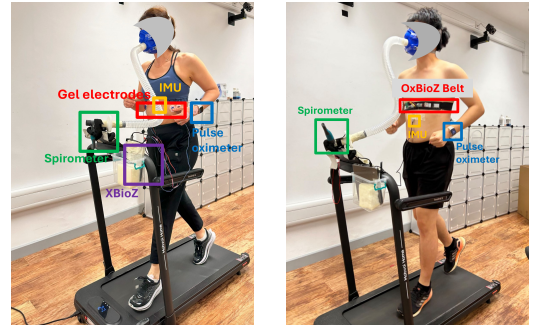


Figure 3: Two different electrode setups are used with OxBioZ hardware. For most of the data collection, gel electrodes were used (left). Our designed wearable electrode belt was also tested (right).

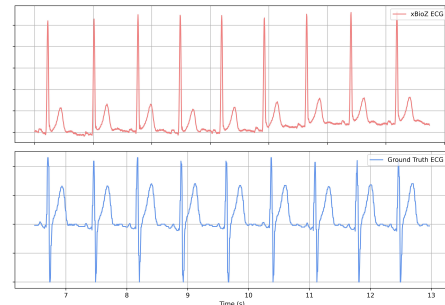


Figure 4: ECG recorded simultaneously by OxBioZ and a reference ECG device. Characteristic waves (P, QRS, T) are clearly visible in OxBioZ measurements.

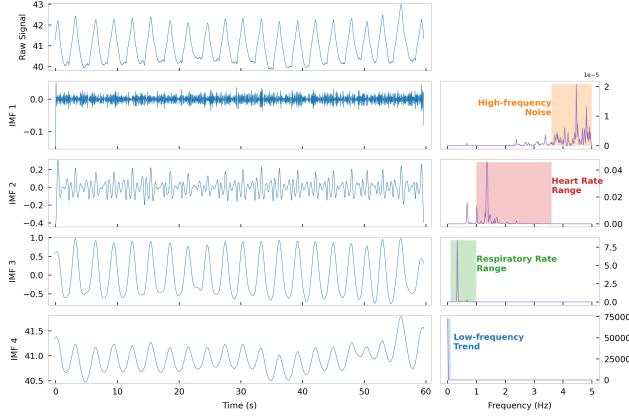


Figure 5: VMD decomposition results. IMF2 corresponds to cardiac activity, IMF3 to respiratory activity, while IMF4 captures slow-varying baseline trends.

5.2 Spectral Analysis for Cardiorespiratory Parameter Estimation

Estimating heart rate (HR) and breathing rate (BR) from wearable signals is a fundamental task in physiological monitoring. To assess the capability of our dataset and device outputs for frequency-domain analysis, we apply Variational Mode Decomposition (VMD) [6] to the raw bioimpedance (BioZ) signals. VMD decomposes an input signal into a predefined set of Intrinsic Mode Functions (IMFs), each representing a narrow-band oscillatory mode, enabling fine-grained separation of overlapping physiological rhythms.

In our setting, the BioZ signal is decomposed into four IMFs: IMF1 captures high-frequency noise components, IMF2 corresponds to cardiac oscillations (1–3.6 Hz), IMF3 reflects respiratory oscillations (0.1–1 Hz), and IMF4 contains slow-varying baseline trends, which may relate to hydration level. The decomposition preserves physiologically interpretable waveforms, demonstrating that the signal quality from the OxBioZ device and dataset is sufficient for precise spectral separation of cardiorespiratory components.

Figure 5 illustrates the decomposition output, where distinct cardiac and respiratory components are clearly resolved. This demonstrates both the effectiveness of VMD in isolating physiological rhythms and the ability of our device and dataset to capture high-quality signals suitable for fine-grained spectral analysis.

5.3 Breathing Volume Estimation

Breathing volume (BV) prediction from wearable sensing data is a representative temporal regression problem in physiological monitoring. To examine whether our dataset and device outputs can support deep learning-based modeling of

such tasks, we implement a baseline study using three representative sequence learning architectures: Recurrent Neural Network (RNN), Long Short-Term Memory (LSTM), and Temporal Convolutional Network (TCN). Each model takes synchronized IMU and BioZ signals as input, augmented with personal attributes (height, weight, sex, age) to account for inter-subject variability. No task-specific feature engineering or architecture tuning is applied, as the objective is to establish a transparent baseline demonstrating the dataset’s applicability to end-to-end temporal modeling.

Table 3 reports the BV estimation performance of the three models in terms of mean absolute error (MAE). These results provide a reference point for future studies exploring more advanced architectures, multimodal fusion strategies, or domain-specific inductive biases using our dataset.

Table 3: BV estimation baseline using deep learning.

Vital sign	Model	MAE ↓
BV (L)	RNN	0.33
	LSTM	0.52
	TCN	0.66

5.4 Total Body Water Estimation

We demonstrate TBW estimation using two baseline approaches, a physics-informed model and a data-driven model.

5.4.1 Physics-Informed Linear Regression.

Building on established bioimpedance theory [5], we derive analytical features that link body geometry and resistance to TBW, and use them within a linear regression framework. Classical studies have shown that $\frac{h_{\text{body}}^2}{R_{\text{body}}}$ is a strong independent predictor of TBW, where h_{body} is subject height and R_{body} the hand-foot AC bioresistance. This follows from modeling lean tissue as a low-resistance conductor:

$$R = \rho_{\text{lean}} \frac{l}{A_{\text{lean}}} = \rho_{\text{lean}} \frac{l^2}{A_{\text{lean}} l} = \rho_{\text{lean}} \frac{l^2}{V_{\text{lean}}},$$

with ρ_{lean} the resistivity of lean tissue, l its length, and A_{lean} its cross-section. Since lean tissue is mostly water, $TBW \approx V_{\text{lean}} = \rho_{\text{lean}} \frac{l^2}{R}$. In our belt configuration, the electrode spacing $d_{\text{elec}} \ll h_{\text{body}}$ measures only the trunk volume

$$V_{\text{lean,elec}}: R_{\text{elec}} = \rho_{\text{lean}} \frac{d_{\text{elec}}^2}{V_{\text{lean,elec}}}$$

If the local tissue water fraction matches the whole-body TBW percentage $TBW\%$, and approximating the body as a cylinder with waist circumference c_{waist} and height h_{body} :

$$TBW\% = \frac{TBW}{V_{\text{body}}} \approx \frac{V_{\text{lean}}}{V_{\text{body}}} \approx \frac{V_{\text{lean,elec}}}{V_{\text{elec}}} \approx \rho_{\text{lean}} \frac{d_{\text{elec}}^2}{R_{\text{elec}} V_{\text{elec}}} \propto \frac{1}{R_{\text{elec}}}$$

$$TBW \approx TBW\% \cdot V_{\text{body}} \propto \frac{c_{\text{waist}}^2 h_{\text{body}}}{R_{\text{elec}}}$$

This scaling term $\frac{c^2h}{R}$, together with PAR, PFA1, PFA2, age, height h , and sex (male:1, female:0), forms the input to a multiple linear regression (MLR):

$$TBW = -59.28 + 2.5057 \cdot 10^{-4} \cdot \frac{c^2h}{R} - 0.3092 \cdot PAR - 0.2134 \cdot PFA1 + 0.7488 \cdot PFA2 + 0.081 \cdot Age + 0.501 \cdot h + 3.6376 \cdot Sex$$

Figure 6 shows predicted vs. ground-truth TBW.

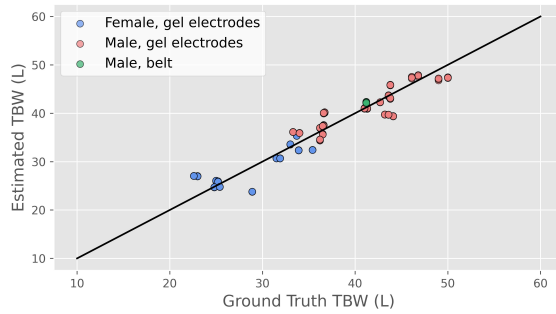


Figure 6: Predicted total body water (TBW) results compared to the ground truth TBW.

5.4.2 Data-Driven End-to-End Learning.

We implement three sequence-based deep learning architectures RNN, LSTM, and TCN in an end-to-end manner. These models serve as baselines for assessing the feasibility of TBW estimation directly from raw measurements, see Table 4.

6 Conclusion

In this study, we addressed the challenge of simultaneous continuous vital sign monitoring and body composition analysis during daily activities by developing the wearable device 'OxBioZ'. Its ability to perform multiple types of bioimpedance analysis and ECG monitoring continuously, while continuously estimating vital signs and TBW during daily activities, has not been achieved previously. Potential application areas include healthcare, athletics, elderly and chronic care, occupational health (e.g., firefighters, miners), and research. The comprehensive dataset created using OxBioZ provides a novel resource for future research on trunk bioimpedance across various tasks.

Table 4: Results of deep learning method for estimating total body water on the data collected by belt.

Vital sign	Model	MAE↓
TBW (L)	RNN	2.11
	LSTM	3.07
	TCN	2.80
	MLR	1.04

With the comprehensive dataset, various future research could be conducted, including on (i) body composition estimation (beyond TBW), (ii) body water volume change estimation, and (iii) human activity recognition.

References

- [1] [n. d.]. AURA Devices. <https://auradevices.io/>. Accessed: 2025-08-15.
- [2] Elisabet Borg and Lennart Kaijser. 2006. A comparison between three rating scales for perceived exertion and two different work tests. *Scandinavian journal of medicine & science in sports* 16, 1 (2006), 57–69.
- [3] Emil Chiauzzi, Carlos Rodarte, and Pronabesh DasMahapatra. 2015. Patient-centered activity monitoring in the self-management of chronic health conditions. *BMC medicine* 13 (2015), 1–6.
- [4] A Cömert, M Honkala, and J Hyttinen. 2013. Effect of pressure and padding on motion artifact of textile electrodes. *BioMed Engineering OnLine* 12, 1 (2013), 26.
- [5] P Deurenberg, K van der Kooy, R Leenen, JA Weststrate, and JC Seidell. 1991. Sex and age specific prediction formulas for estimating body composition from bioelectrical impedance: a cross-validation study. *International journal of obesity* 15, 1 (January 1991), 17–25.
- [6] K Dragomiretskiy and D Zosso. 2013. Variational mode decomposition. *IEEE trans. on signal processing* 62, 3 (2013), 531–544.
- [7] K Guk, G Han, J Lim, K Jeong, T Kang, E-K Lim, and J Jung. 2019. Evolution of wearable devices with real-time disease monitoring for personalized healthcare. *Nanomaterials* 9, 6 (2019), 813.
- [8] T Hao, C Bi, G Xing, R Chan, and L Tu. 2017. MindfulWatch: A smartwatch-based system for real-time respiration monitoring during meditation. *Proc. of the ACM on Interactive, Mobile, Wearable and Ubiquitous Technologies* 1, 3 (2017), 1–19.
- [9] KJ Higgins. 2004. *Validation of bioimpedance spectroscopy to assess acute changes in hydration status*. Ph.D. Dissertation. Univ. of Arizona.
- [10] Michel Y Jaffrin and Hélène Morel. 2008. Body fluid volumes measurements by impedance: A review of bioimpedance spectroscopy (BIS) and bioimpedance analysis (BIA) methods. *Medical engineering & physics* 30, 10 (2008), 1257–1269.
- [11] Panagiotis Kassanos. 2021. Bioimpedance Sensors: A Tutorial. *IEEE Sensors Journal* 21, 20 (2021), 22190–22219.
- [12] Sami F Khalil, Mas S Mohktar, and Fatimah Ibrahim. 2014. The theory and fundamentals of bioimpedance analysis in clinical status monitoring and diagnosis of diseases. *Sensors* 14, 6 (2014), 10895–10928.
- [13] Y Lee, JW Chung, GH Lee, H Kang, J-Y Kim, C Bae, H Yoo, S Jeong, H Cho, S-G Kang, et al. 2021. Standalone real-time health monitoring patch based on a stretchable organic optoelectronic system. *Science Advances* 7, 23 (2021), eabg9180.
- [14] Heather Lukas, Changhao Xu, You Yu, and Wei Gao. 2020. Emerging telemedicine tools for remote COVID-19 diagnosis, monitoring, and management. *ACS nano* 14, 12 (2020), 16180–16193.
- [15] Henry C Lukaski, Nicanor Vega Diaz, Antonio Talluri, and Lexa Nescolarde. 2019. Classification of hydration in clinical conditions: indirect and direct approaches using bioimpedance. *Nutrients* 11, 4 (2019), 809.
- [16] S McGee. 2012. Chapter 36 - palpation of the heart. In *Evidence-based physical diagnosis*. W.B. Saunders, Philadelphia, 309–319.
- [17] Christina Orphanidou. 2017. Signal quality assessment in physiological monitoring: state of the art and practical considerations. (2017).
- [18] J Rosell, J Colominas, P Riu, R Pallas-Areny, and JG Webster. 1988. Skin impedance from 1 Hz to 1 MHz. *IEEE Trans. on Biomed. Eng.* 35, 8 (1988), 649–651.

Received 18 August 2025; accepted 10 September 2025